

## Numerical analysis of thermal and composite stresses in pre-stressed concrete pavements

Fereidoon Moghadas Nejad<sup>1</sup>, Sepehr Ghafari<sup>\*1</sup> and Shahriar Afandizadeh<sup>2</sup>

<sup>1</sup>Department of Civil and Environmental Engineering, Amirkabir University of Technology, Tehran, Iran

<sup>2</sup>Department of Civil and Environmental Engineering, University of Science and Technology, Tehran, Iran

(Received January 14, 2012, Revised June 25, 2012, Accepted July 3, 2012)

**Abstract.** One of the major benefits of the pre-stressed concrete pavements is the omission of tension in concrete that results in a reduction of cracks in the concrete slabs. Therefore, the life of the pavement is increased as the thickness of the slabs is reduced. One of the most important issues in dealing with the pre-stressed concrete pavement is determination of the magnitude of the pre-stress. Three dimensional finite element analyses are conducted in this research to study the pre-stress under various load (Boeing 777) and thermal gradient combinations. The model was also analyzed under temperature gradients without the presence of traffic loading and the induced stresses were compared with those from theoretical relationships. It was seen that the theoretical relationships result in conservative values for the stress.

**Keywords:** thermal stress; pre stressed concrete pavement; finite element

---

### 1. Introduction

The use of pre-stressed concrete pavements has received considerable attention for years as a measure for extending the service life of pavements yet remaining cost-effective.

It is well understood that conventional concrete pavements are designed taking into account the fundamental flexural and tensile weakness of concrete slabs. In pre-stressed concrete pavements the pre-compression induced by pre-stressing, results in greater allowable flexural and tensile stresses which can lead to a reduced design thickness for the concrete slabs as well as an increased service life in comparison with the conventional concrete pavements.

#### 1.1 Stresses arising from curling by means of the equations

Curling as well as warping are two major environmental loadings that induce stresses in rigid pavements. Curling happens to most slabs on grade which is brought about primarily due to the temperature gradient between the top and bottom of the slab. The temperature difference induces an upward curling moment to the slab which causes the top surface to deflect upwards. The stresses in concrete pavements are analyzed using the Westergaard equations (Delatte 2008, Huang 1993)

---

\*Corresponding author, Ph.D candidate, E-mail: [sepehr@aut.ac.ir](mailto:sepehr@aut.ac.ir)

$$-\frac{\partial^2 z}{\partial x^2} = \frac{12}{Eh^3}(M_x - \nu M_y) + \frac{\alpha_t \Delta T}{h} \quad (1)$$

$$-\frac{\partial^2 z}{\partial y^2} = \frac{12}{Eh^3}(M_y - \nu M_x) + \frac{\alpha_t \Delta T}{h} \quad (2)$$

$$-\frac{\partial^2 z}{\partial x \partial y} = \frac{12}{Eh^3}(1 + \nu)M_z \quad (3)$$

Where

$E$  = concrete elastic modulus (psi),

$h$  = slab thickness (in),

$\nu$  = Poisson's ratio of concrete,

$\alpha_t$  = thermal expansion coefficient ( $^{\circ}\text{F}$ ),

$\Delta T$  = top and bottom temperature difference of the slab ( $^{\circ}\text{F}$ ),

$M_x$  = moment about the X axis,

$M_y$  = moment about Y-axis,

$M_z$  = moment about Z-axis.

If the slab is considered to be infinite in two directions for a point with a specific distance from the edge of the slab (Delatte 2008)

$$M_x = M_y = \frac{Eh^2 \alpha_t \Delta T}{12(1-\nu)} \quad \text{and} \quad M_z = 0 \quad (4)$$

Dividing Eq. (4) by the section modulus; the stress is obtained by the following Eq. (5)

$$\sigma_0 = \frac{E \alpha_t \Delta T}{2(1-\nu)} \quad (5)$$

In the AASHTO road test, the average maximum standard difference in June and July for downward curling was  $10.2^{\circ}\text{C}$  and for upward curling was  $-4.9^{\circ}\text{C}$ . It was reported that the mentioned temperatures are respectively related to  $0.07^{\circ}\text{C}/\text{mm}$  and  $0.03^{\circ}\text{C}/\text{mm}$  gradients (Huang 1993).

### 1.2 Properties of the pre-stressed concrete pavements

Based on the AASHTO recommendation, it is suggested that the pre-stressed pavement thickness should be %65 the thickness of a conventional concrete pavement thickness which should be at least 150 mm (AASHTO 1993). AASHTO pavement guide recommends a minimal thickness of 100 to 150 mm for pre-stressed concrete pavements. Various observations and researches show that even though the pre-stressed concrete slabs are constructed with lengths of 180 to 210 m (FAA 2009), the common length for the pre-stressed concrete slab length is 150 m. The slab width variations depend on the construction conditions. Usually it has a minimum of 7.6 m (AASHTO 1993, Hancock *et al.* 2000). Minimum thickness for the base layer is 150 mm according to AASHTO pavement design guide but in some cases thicknesses equal to 100 mm are also applied. It is suggested that a layer for reducing the friction between the pre-stressed concrete slab

and the base layer be used which consists of two Polyethylene surfaces with a thickness of 15 to 20 mm (Merritt *et al.* 2005).

### 1.1.1 The theory behind the pre-stressed pavements

The main concept in the design of pre-stressed concrete pavements is that the concrete has a greater compressive strength than tensile strength (FAA 2009, Hancock *et al.* 2000, Merritt *et al.* 2005).

According to this, the slab thickness can be reduced if a pre-stressed pavement is constructed (Merritt *et al.* 2005). The principal design formula for this type of pavement is (Hancock *et al.* 2000)

$$f_t + f_p \geq f_{\Delta t} + f_f + f_l \quad (6)$$

Where  $f_t$  is the allowable concrete flexural stress,  $f_p$  is the concrete pre-stress,  $f_{\Delta t}$  is the curling stress due to thermal gradient,  $f_f$  is stress due to pavement friction and  $f_l$  is stress due to traffic loading.

The curling stress in concrete is obtained from (5) (NCHRP 2001).

For a slab with a length less than 220 m, the friction stress between the concrete slab and the underlying layer in the direction of the slab length or width is determined by using (7) (AASHTO 1993, Hancock *et al.* 2000)

$$f_f = \frac{C \cdot \gamma \cdot L}{2 \times 144} \quad \text{or} \quad f_f = \frac{C \cdot \gamma \cdot W}{2 \times 144} \quad (7)$$

Where:

$C$  = pavement friction coefficient,

$L$  = slab length (ft)

$W$  = slab width

$\gamma$  = specific weight (pcf).

A value of 0.6 for the coefficient of friction is recommended to be appropriate based on experiments (UFC 2001).

The main purpose of this research is to evaluate thermal and composite stresses on the pre-stressed concrete pavement systems and acquire a realistic understanding of the pavement operation under thermal stresses. Therefore, it is tried to recognize the defects in the equations and relative assumptions used in predicting the behavior of this type of pavement. Thus, a three dimensional finite element model of the pre-stressed concrete pavement was prepared and analyzed.

## 2. Modeling

### 2.1 Model verification

In order to verify the modeling procedure, a sample concrete pavement which was constructed and instrumented in the field was analyzed using the same modeling procedure in the software. The analysis output was compared to the values obtained in the field.

Table 1 Curling and thermal differential measurements (Zahidul *et al.* 2003)

Day Time	August 7		September	
	Curling (mils)	Temp. Diff. (°F)	Curling (mils)	Temp. Diff. (°F)
8 am	-	-9.0	-2.008	-9.0
9 am	-0.984	-5.4	-5.000	-5.4
10 am	-2.992	0.9	-0.402	-0.9
11 am	-2.008	7.2	-2.008	2.7
12 am	0.984	12.6	2.008	9.9
1 pm	10.984	18.9	7.992	16.2
2 pm	14.016	21.6	12.992	20.7
3 pm	25.00	22.5	22.992	23.4
4 pm	20.984	20.7	20.000	24.3
5 pm	17.992	18.0	15.984	21.6
6 pm	15.000	14.4	12.992	17.1
7 pm	12.992	9.9	12.992	11.7

### 2.1.1 Test section

The test section was a jointed plain concrete pavement section on interstate 70, constructed in summer 2003 in Kansas (Zahidul *et al.* 2003). This section consisted of two passing lanes, each having a width of 3.6 m, the two internal (left) and external (right) shoulders are respectively 1.8 and 3.0 m width. Joint spacing is 5 m and the Dowel bars have a diameter of 37.5 mm at a 300 mm distance from each other for transferring loads. The pavement cross section contains a concrete slab with a thickness of 300 mm, a 100 mm base layer and a 150 mm lime stabilized subgrade. The average 28 day compressive strength of the concrete is 36 MPa and the 3 day rupture modulus is 3968 kpa.

### 2.1.2 Temperature difference and curling measurements

The curling and thermal differentials measured in the test section between top and bottom of the concrete slab are presented in Table 1.

### 2.1.3 Finite element modeling

Eight node brick/solid elements were utilized to model the concrete slab as well as the underlying layers (base, subgrade).

Interface elements (also known as the contact pairs) are used to model the interface between the concrete slab and the granular base layer.

Three dimensional beam elements were used to model the load transfer between the slabs based on the linear elastic joint concept (David 1998, Moghadas Nejad *et al.* 2008). An equivalent shear stiffness,  $K_{joint}$ , based on the concept was considered for the joints which is obtained by (8)

$$K_{joint} = \frac{5EI}{(1 + \mu)\delta h^2} \quad (8)$$

Where:

$h$ : Height of the beam element

EI: Required beam stiffness (per unit length of joint)

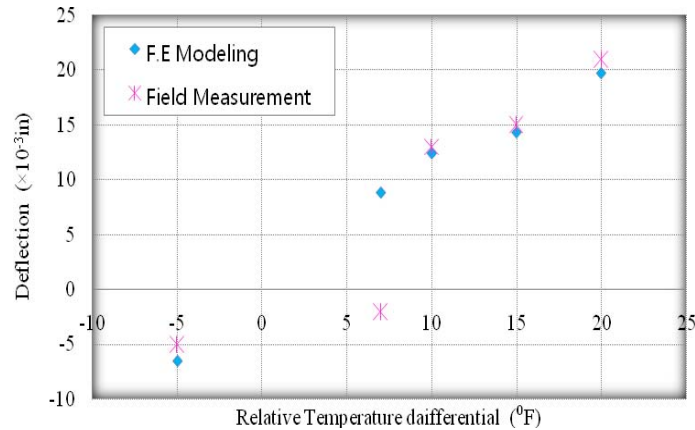


Fig. 1 Comparison between maximum curling from the model and the field test

$\mu$  : Poisson’s ratio for the beam material

$\delta$  : Joint width (beam span)

**2.1.4 Material properties**

All the layers except the subgrade were modeled with linear elastic behavior. The material properties are as follows: the Young’s modulus of concrete, steel, base, and subgrade are respectively equal to  $2.9 \times 10^4$ ,  $2.0 \times 10^5$ ,  $6.5 \times 10^3$  and 275 MPa, Poisson's ratio of the concrete layer, base, subgrade and the dowel bars are respectively 0.15, 0.15, 0.2 and 0.25. Concrete and steel thermal expansion coefficients are  $9.0 \times 10$  and  $11.7 \times 10^{-6}$  mm/mm/°C respectively.

**2.1.5 Subgrade modeling**

In order to model the elastic-plastic behavior of the subgrade soil the Drucker-Prager yield criterion which is a commonly used material model for simulating the elastic-plastic behavior of soils, rocks, concrete, etc. (Xia *et al.* 2001, Peng *et al.* 2009) is used for modeling the material. Fig. 4 represents the yield criterion and its shape for the Drucker-Prager model. The required input data for the model are the soil cohesion and internal friction angle that are input equal to 0.16 kpa and 45 degrees respectively in this research.

**2.1.6 Model loading**

The model was thermally loaded by temperature profiles acquired from field. Thermal loads were applied on different points throughout the slab thickness. Temperature differentials chosen for thermal loading are: -7°C, -10°C, -12°C, -14°C and -20°C.

**2.1.7 Comparison between field test results and model analysis outputs**

Fig. 1 shows the maximum concrete slab deflection obtained by the numerical modeling and those from the field tests. A fair agreement is seen between the field deflections and those from the analysis.

**2.2 Modeling the pre-stressed concrete pavement**

Table 2 Applied material properties in finite element model

Layer	Property	Value
Concrete slab	Elastic modulus (MPa)	27500
	Poisson's ratio	0.15
	Specific Weight (Kg/m)	2400
	Thermal expansion coefficient (mm/c)	$10 \times 10^{-6}$
Base	Elastic modulus (MPa)	3450
	Poisson's ratio	0.2
	Specific Weight (Kg/m)	2100
Subgrade	Elastic modulus (MPa)	103.5
	Poisson's ratio	0.4
	Specific Weight (Kg/m)	2040

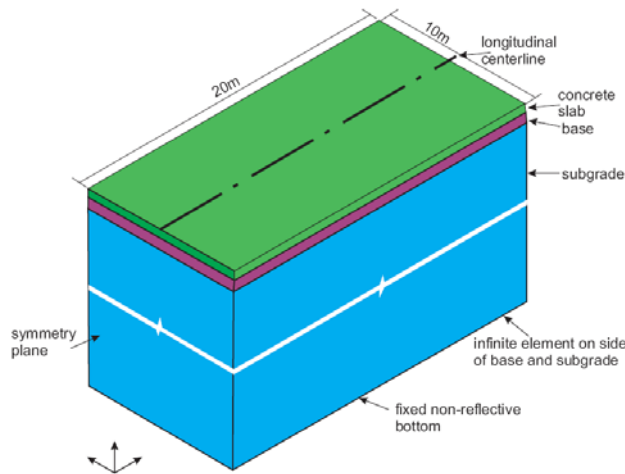
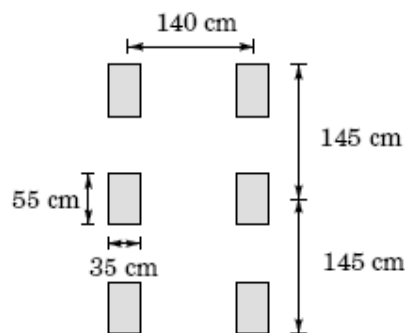


Fig. 2 Finite element model with the boundary conditions



B777-200 aircraft tridem  
Tire pressure = 1.5 MPa

Fig. 3 Dimensions and tire-contact areas (Tacıroglu *et al.* 1998)

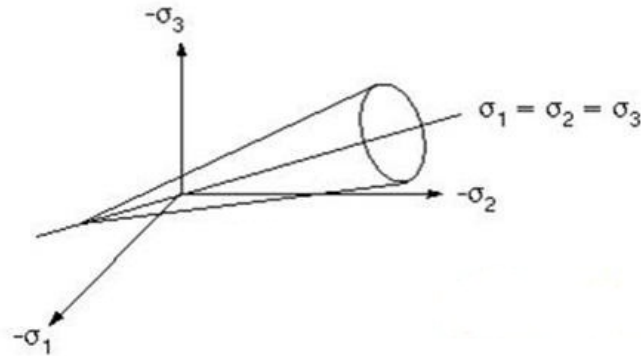


Fig. 4 3-D representation of the Drucker-Prager yield criterion

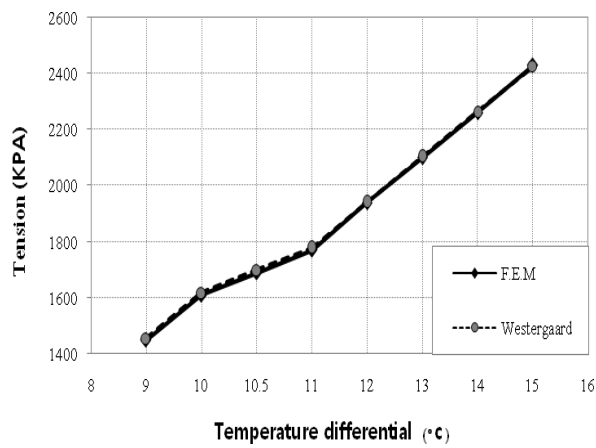


Fig. 5 Comparison of stresses between the model analysis and the Westergaard formula (slab thickness=150 mm)

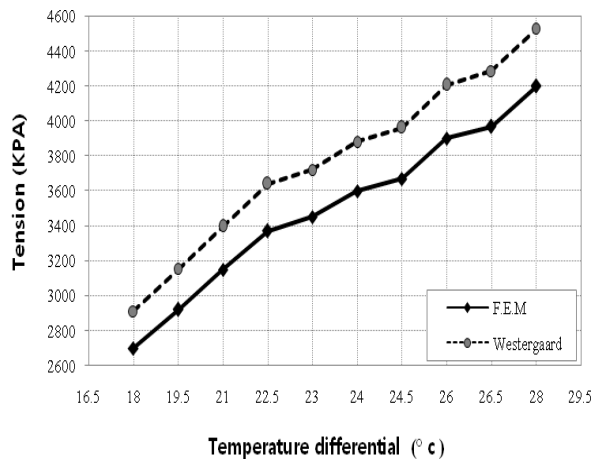


Fig. 6 Comparison of stresses between the model analysis and the Westergaard formula (slab thickness=400 mm)

Eight node brick/solid elements were used to model the concrete slab as well as the underlying layers.

The concrete slab length and width are considered 20 m and 10 m respectively and the thickness of the subgrade is equal to 8 m in the finite element model. Concrete slab thickness varies from 150 mm to 400 mm.

### 2.2.1 Material properties

Material characteristics are as listed in Table 2.

### 2.2.2 Loading the model

Symmetric boundary conditions are considered for the base and the subgrade layers (Fig. 2). The concrete slab is considered to be jointed and discontinuous.

The composite load consists of Boeing 777 tire loads and thermal loading. The latter is positive gradient from 6 C/mm to 8 C/mm by a %5 correspondence and the negative gradient is equal to 27, 33 and 4 C/mm. When a traffic load and negative thermal gradient is applied as a composite loading, the critical condition occurs when the load is located at the transverse edge of the concrete slab. In a composite loading with the positive gradient, critical condition occurs when the load is located at the middle of the slab length. Fig. 3 shows the dimensions and the effective area of Boeing 777 tires.

### 2.2.3 The process of modeling the pre-stress

The pre-stress should be in longitudinal and transverse directions of the concrete layer. In order to create the mentioned conditions, the pre-stress was applied as surface pressure on the surface edges of the concrete slab.

## 3. Results and discussions

### 3.1 Comparison of thermal stresses from the analysis and theory

Figs. 5 and 6 present thermal stress comparison graphs between the numerical analysis results and those from the Westergaard relationship for slabs with thicknesses of 150 mm and 400 mm.

The Westergaard equation results in higher values of thermal stress than those obtained by the finite element analysis as the slab thickness is increased. It has also been shown in other similar researches that the Westergaard equations overestimate thermal stress values as the slab thickness is increased, the main causes of this overestimation is associated with the assumption of the linear thermal gradient throughout the slab thickness as well as the consideration of the concrete slab as a plate on an elastic foundation (Shimomura *et al.* 2008). In the finite element analyses, as implemented here, nonlinear temperature distributions can be applied to the model and the simplification resulted from assuming a linear elastic behavior for the underlying soil layers is substituted by a more realistic–nonlinear elastic plastic behavior as in the applied Drucker-Prager model- behavior. The stress values resulted from the Westergaard equation in the worst state (at positive thermal gradient condition) are 7.8% greater than those of the model analysis. These values will be decreased to 1.2% in the case of negative thermal gradient.

### 3.2 Primary analyses and determination of the pre-stress

Table 3 Primary pre-stresses (kPa)

Pre-stressed Slab Thickness (mm)	150	200	250	300	350	400
Longitudinal	4590	4160	3510	3860	2380	1680
Transverse	5070	4530	3970	3230	2870	1960

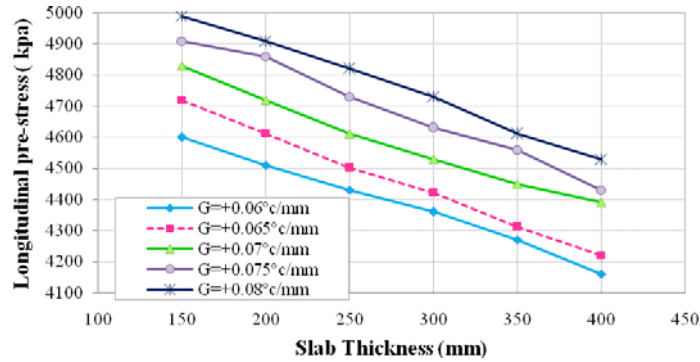


Fig. 7 Longitudinal pre-stress in the slab under airplane tire composite load and positive thermal gradient

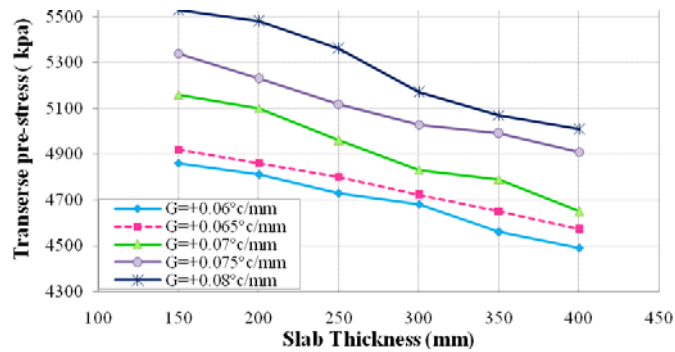


Fig. 8 Transverse pre-stress in the Slab under airplane tire composite load and positive thermal gradient

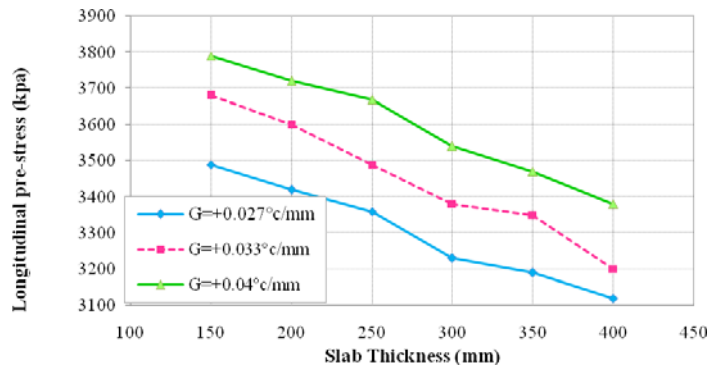


Fig. 9 Longitudinal pre-stress in the slab under airplane tire composite load and negative thermal gradient

In order to obtain a reasonable estimation of the required pre-stress for each of the concrete slab thicknesses, the models were analyzed under the airplane wheel load. The resulted values for the pre-stress are given in Table 3.

### 3.3 Effect of the magnitude of the pre-stress on the slab thickness

Pre-stress values under composite loading are shown in Figs. 7 to 10.

The pre-stress is reduced by 9.6% and 8.5% in the transverse and longitudinal directions as the thickness of the concrete slab is increased under a composite load consisting of a positive thermal gradient and airplane wheel load.

The increase in the slab thickness results in a reduction of the pre-stress by 11.5% in both directions under the composite loading with a negative thermal gradient.

### 3.4 Compressive stress on top of the subgrade

The maximum stress on top of the subgrade was also obtained by the finite element analysis. The stress variation trend is presented in Figs. 11 and 12.

It can be seen that increasing the thickness causes a reduction in the compressive stress on top of subgrade. The main reason is the enhanced stress distribution in the pavement system as a result of the increase in the concrete slab thickness causing the reduction of the compressive stress transferred to the subgrade level. Under a positive thermal gradient, increase in slab thickness from 150 mm to 400 mm reduces the compressive stress by 35%. A 32% reduction is seen for the negative gradient.

### 3.5 Determination of the ultimate pre-stress and generating the design equation

#### 3.5.1 Estimation of the number of aircraft load repetitions

PCA recommended Eq.s are used in this research to study the allowable number of load repetitions. The allowable number of load repetitions is calculated as follows (Huang 1993)

$$\frac{\sigma}{R} \geq 0.55 \quad \log N_f = 11.737 - 12.022 \left( \frac{\sigma}{R} \right) \quad (9)$$

$$0.45 < \frac{\sigma}{R} < 0.55 \quad N_f = \left( \frac{4.2577}{\left( \frac{\sigma}{R} \right) - 0.4325} \right)^{3.268} \quad (10)$$

$N_f$  is considered to be unlimited for  $\sigma / R \leq 0.45$ .

Where:

$\sigma$  = flexural stress in slab (kPa)

$N_f$  = allowable number of repetitions

$\alpha$  = bending stress in the slab (kPa),

$R$  = concrete modulus of rupture (kPa).

According to the principal design Eq. for the pre-stressed concrete pavements and considering the load repetition coefficient the following equation rules (UFC 2001)

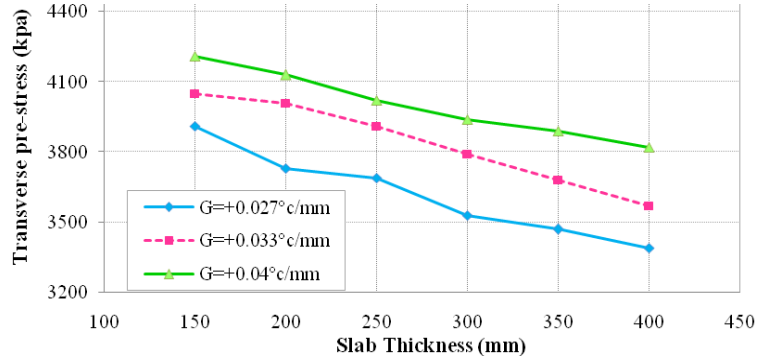


Fig. 10 Transverse pre-stress in the slab under airplane tire composite load and negative thermal gradient

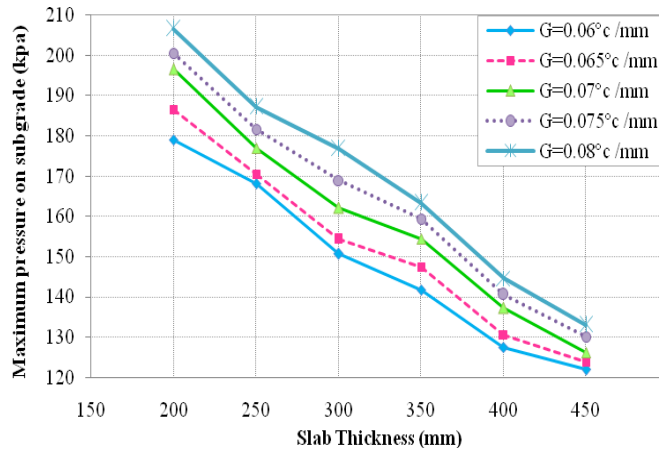


Fig. 11 Compressive stress on top of the subgrade under composite load at positive thermal gradient

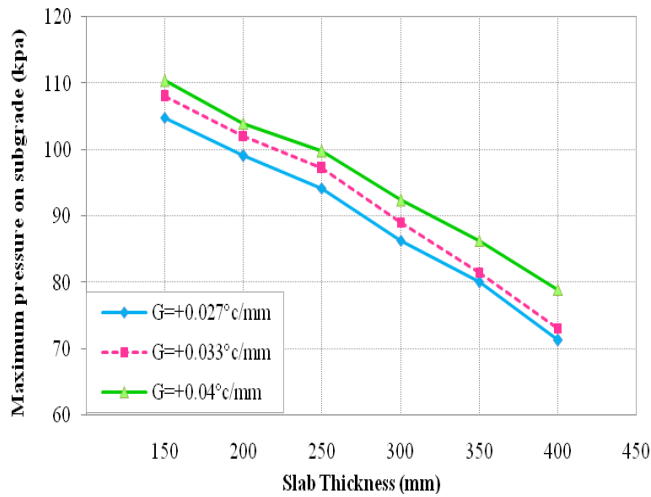


Fig. 12 Compressive stress on top of the subgrade under composite load at negative thermal gradient

$$d_s = r_s + r_t + f_1 - nR \quad (11)$$

Where

$d_s$  = pre-stress

$R$  = concrete allowable bending strength

$r_s$  = stresses arising from friction between the slab and the base layer

$r_t$  = curling stress arising from thermal Gradient between the concrete slab surface and below,

$f_1$  = bending stress arising from airplane wheel load and

$n$  = allowable stress ratio for the number of load repetitions.

### 3.6 Calculating the ultimate pre-stress values

In order to determine the required ultimate pre-stress under the composite loading (Boeing 777, thermal gradient and friction stresses) the pre-stress obtained in the current research can be used. Consequently, knowing the thermal gradient and referring to Figs. 7 to 10, the overall pre-stress is determined and the friction stress is also calculated considering the dimensions of the slab according to Eq. (7) finally, the ultimate pre-stress along the longitudinal and transverse directions are determined by means of the allowable number of load repetitions and the concrete modulus of rupture (using Eqs. (12) and (13)).

$$d_{slf} = d_{sls} + r_{sl} - nR \quad (12)$$

$$d_{swf} = d_{sws} + r_{sw} - nR \quad (13)$$

Where

$d_{slf}$  = ultimate longitudinal pre-stress, and

$d_{swf}$  = ultimate transverse pre-stress (kPa).

$d_{sls}$  = overall longitudinal pre-stress and

$d_{sws}$  = overall transverse pre-stress(kPa).

Hence, for the slab with a length of 20 m and a width of 10 m, as pointed out in Section 3.2, the frictional stresses will be

$$r_{sl} = \frac{0.6 \times 2400 \times 20}{2} = 14400 \text{ kg / m}^2 = 283 \text{ kpa}$$

$$r_{st} = \frac{0.6 \times 2400 \times 10}{2} = 7200 \text{ kg / m}^2 = 71 \text{ kpa}$$

For an allowable concrete flexural strength of 30 MPa

$$R = 0.6\sqrt{30} = 3.3 \text{ Mpa} = 3300 \text{ kpa}$$

Therefore, Eqs. (14) and (15) will be as follows

$$d_{slf} = d_{sls} + 283 - 3300n \quad (14)$$

$$d_{swf} = d_{sws} + 71 - 3300n \quad (15)$$

In which  $d_{sls}$  and  $d_{sws}$  are acquired from Figs. 7 to 10.  $n$  is determined by Eqs. (9) or (10) and the ultimate pre-stress will be calculated.

#### 4. Conclusions

- According to the analyses, the Westergaard equations generally result in greater thermal stresses in comparison with the values obtained from the numerical analyses. Regarding the defects in the Westergaard equations (consideration of a linear thermal gradient, consideration of the concrete slab as a plate on elastic foundation, etc.) the presented finite element analysis and results can be used as a reliable alternative to the results obtained from the Westergaard equations.

- Under composite loading consisting of thermal gradient and airplane wheel load, as the prestressing force is increased, the required concrete thickness is reduced. In other words, having a specific slab thickness, the magnitude of the induced pre-stress can be determined by Figs. 7 to 10 and it has an inverse relationship with the slab thickness.

- The required pre-stress under composite loading is different in longitudinal and transverse directions; that has to be considered in channelized movements of the aircraft such as in runways.

- A defect in the FAA equation is that a tandem axle load with three wheels is not considered. This load case is considered by the application of Boeing 777 loading in this research.

#### References

- AASHTO guide for design of pavements (1993), *Published by the American association of state highway and transportation officials*.
- David, R.B. (1998), *Development of advanced computational models for airport pavement design-DOT/FAA/AR-97/47*, Federal Aviation Administration, Washington DC.
- Delatte, N. (2008), *Concrete pavement design, construction and performance*, Taylor & Francis, New York.
- Hancock, J. and Hossain, M. (2000), "Cross-tensioned concrete pavement: An alternative modern PCCP design", *Mid-Continent Transportation Symposium Proceedings*, 207-210.
- Huang, Y.H. (1993), *Pavement analysis and design*, Prentice Hall, New Jersey.
- Merritt, D.K., McCullough, B.F. and Burns, N.H. (2005), "Design-construction of a precast prestressed concrete pavement for interstate 10", *PCI J.*, **50**(2), 18-27.
- Moghadas Nejad, F. and Ghafari, S. (2008), "Numerical analysis of concrete overlays on flexible pavements", *9<sup>th</sup> International Conference on Concrete Pavements*, 647-658.
- NCHRP Guide for Mechanistic-Empirical Design of New and Rehabilitated Pavement Structures (2001), *APPENDIX KK*.
- Peng, Y. and He, Y. (2009), "Structural characteristics of cement-stabilized soil bases with 3D finite element method", *Front. Architect. Civil Eng. China.*, **3**(4), 428-434.
- Federal Aviation Administration. (2009), *Prestressed concrete pavement design*, Chapter 6, TM5-825-3/AFM 88-6.
- Shimomura, T., Nishizawa, T. and Ozeki, T. (2008), "Evaluation of thermal stress in airport concrete pavement slab by 3D-FEM analysis", *9<sup>th</sup> International Conference on Concrete Pavements*, 740-754.
- Tacioglu, E. (1998), *Constitutive modeling of the resilient response of granular solids*, Thesis for the Degree of Doctor of Philosophy, university of Illinois.
- Unified Facilities Criteria (UFC). (2001), *Pavement design for airfields*.
- Xia, K. (2011), "Large deformation finite element model for soil compaction", *J. Geotech. Geoen.*, **7**(2), 123-137.

Zahidul, Q.S. and Hossain, M. (2003), *Temperature and curling measurement on concrete pavement*, Department of civil engineering, Kansas University.

*CM*